Precise Extraction of Geometrical Dependence from Solar Wind Columnar Turbulence Measurements

A. L. Berman
TDA Engineering Office

Experimental solar wind columnar turbulence measurements have frequently been modelled as a function of a single geometrical parameter. Since columnar turbulence results from the signal path integration of an appropriate source function, hypothesized columnar turbulence models must be cast as a function of two independent geometrical parameters. This article quantifies the distortion which results from the attempt to extract and model the functional dependence of experimental columnar turbulence measurements via usage of a single geometrical parameter.

In the case of Doppler phase fluctuation data (ϕ), the net effect of usage of a single geometrical parameter is to translate the more accurate two parameter formulation:

$$\phi(a, \beta) \cong K\beta a^{-1.3}$$

where:

a = signal closest approach distance

β = Earth-Sun-probe angle

to a less accurate one parameter expression of the form:

$$\phi(a) \approx K a^{-1.5}$$

I. Introduction

Precise determination of the functional (geometrical) dependence of solar wind columnar turbulence from experimental measurements is required by solar wind investigators for the validation of theoretical derivations. Directly, experimental turbulence measurements can be used to confirm the (hypothesized) process by which such turbulence is generated; subsequently, by inverting this process, the measurements can be made to yield valuable information about the geometrical dependence of the most basic solar wind parameters, such as electron density and solar wind velocity. In the early days of solar wind research, it was understandable that solar wind turbulence would be measured solely as a function of the dominant geometrical parameter – elongation angle (or, equivalently, Sun-Earth-probe angle or signal path closest approach distance). However, some recent work as well (Woo, Ref. 1; Callahan, Ref. 2) has continued to rely on a single (geometrical) parameter in the extraction of the geometrical dependence of solar wind columnar turbulence. Given today's more sophisticated measurement environment, more exact functional dependence determinations are highly desirable.

Ultimately, all measurements of columnar turbulence must be modelled as or mapped back to the signal path integration of some (possibly complex) solar wind parameter. There is as yet no consensus on the proper theoretical treatment which identifies such a parameter. However, excellent results have been obtained by empirically modelling columnar turbulence as the signal path integration of electron density (Berman, et al. Ref. 3). It has been shown (Berman, et al. Ref. 4) that the signal path integration of a power-law electron density model can be accurately described in closed form in terms of two geometrical parameters – Sun-Earth-probe angle α and Earth-Sun-probe angle β. Significant "distortions" occur if one attempts to determine (power law) radial dependence of solar wind turbulence via usage of only one geometrical parameter, rather than the two that are required for a complete geometrical description. Such distortions mask the process whereby solar wind turbulence is generated, and can lead to erroneous inferences in regard to the functional dependence of the basic solar wind parameters (e.g., density and velocity).

This article will attempt to quantify the distortions induced via usage of an incomplete geometrical description. Included in the discussion are the cases of both close (spacecraft) and distant (natural) signal sources.

II. Close Signal Sources

There is now considerable evidence that all measurements of columnar turbulence[1] strongly correlate with signal path integrated or in situ electron density; interplanetary scintillation examples are Erskine, et al. (Ref. 5), Chang (Ref. 6), and Houminer, et al. (Ref. 7); phase fluctuation examples are Berman, et al. (Ref. 3) and Berman (Refs. 8, 9, and 10); spectral broadening, Rockwell (Ref. 11). Since the indications for integrated electron density correlation are so obvious, the discussion here will be structured within such a framework. Were it to turn out, however, that columnar turbulence is really better represented by the signal path integration of a complex parameter related to but not identical to electron density, the argument for a complete geometrical description would continue with equal validity.

A simple example serves to motivate an appreciation of the problem, when the (spacecraft) source is near the closest approach point (the "near-source" limit). At (different) times during 1975-1976 the Sun-Earth-probe angle α and Earth-Sun-probe angle β for several spacecraft were as follows:

Spacecraft	α, deg	β, deg
Helios 1	17.5	90
Viking	17.5	152
Pioneer 10	17.5	160

As is schematically illustrated in Fig. 1, all three spacecraft are at the identical Sun-Earth-probe angle of 17.5 deg (or signal closest approach distance of 65 solar radii), so that *all else being equal*, an experimentor relying solely on signal closest approach distance a might expect all (signals) to display a similar level of turbulence. However, since integrated density (as will be shown) scales with β, there will be a systematic difference of approximately 80% in the turbulence levels between the two extremes (the Helios 1 and Pioneer 10 cases). It is thus of interest to quantify in some manner the distortion induced via reliance on a single geometrical parameter.

In Ref. 12, Berman et al., have found a very large volume of Viking two-way S-band Doppler phase fluctuation data (ϕ) to be consistent with the signal path integration of $Kr^{-2.30}$ for $r \geqslant 5r_o$, where r = radial distance and r_o = solar radius. This results in the following approximate expression (Ref. 4):

$$\phi(\alpha,\beta) \cong K\beta(\sin\alpha)^{-1.3}\,F(\alpha,\beta)$$

where:

ϕ = Doppler phase fluctuation

K = constant

β = Earth-Sun-probe angle

α = Sun-Earth-probe angle

$$F(\alpha,\beta) = 1 - 0.05\left\{\frac{\left(\beta - \frac{\pi}{2} + \alpha\right)^3 - \left(\alpha - \frac{\pi}{2}\right)^3}{\beta}\right\} - 0.00275\left\{\frac{\left(\beta - \frac{\pi}{2} + \alpha\right)^5 - \left(\alpha - \frac{\pi}{2}\right)^5}{\beta}\right\}$$

Since $F(\alpha, \beta)$ is only a weak function of α and β, one further approximates the above as:

$$\phi(\alpha,\beta) \cong K\beta a^{-1.3}$$

[1]With the exception of angular broadening, which is not considered here due to an insufficiency of consistent data, and Faraday rotation, which measures the signal path integration of the product of electron density and the magnetic field.

where the (equivalent) signal closest approach distance a has been substituted for sin α. The important point of the above expression is that even starting with a power-law source function (in this case, density), the resulting integrated columnar turbulence departs significantly from power-law (with a). An extreme example of the effect of changing β on turbulence which is modelled only as a function of a is the Helios data at approximately 65 r_o as seen in Fig. 2. The large, nearly vertical, fall-off of the data at 65 r_o is due to the rapid change in β as Helios 1 underwent perihelion, and not to any significant variation with a.

To be able to roughly compare results obtained through use of a single geometric parameter to those based on a complete (two-parameter) geometrical description, an approximate "*total*" radial dependence will be constructed by rewriting:

$$\phi(a,\beta) \cong K\beta a^{-1.3}$$

as:

$$\phi(a,\beta) \cong Ka^{-1.3 + \ell n\beta/\ell na}$$

or

$$\phi(a) \approx Ka^{-1.3 + \ell n\,(\beta_1/\beta_2)/\ell n\,(a_1/a_2)}$$

where the subscripts 1 and 2 define the applicable (radial) span of data. Since the relationship between β and a is definitely *not* power law, consideration of the "total" (power law) radial dependence permits only a rough idea as to the expected distortion to be encountered in relying on a single geometric parameter.

Table 1 presents examples of the expected total radial dependence from the signal path integration of a $Kr^{-2.30}$ electron density source, for actual spacecraft geometries during 1975-1976. From Table 1, it is apparent that one might expect to find a "total" radial dependence of:

$$\phi(a) \approx a^{-1.5}$$

from a typical set of such data.

III. Distant Signal Sources

Distant signal sources require the same two-parameter geometrical description as do close signal sources. In this case though, it is Earth which approaches the signal closest approach point ("near-Earth" limit), rather than the source, as discussed in section II. In either case, however, the effect is always most pronounced in the region where $\beta \sim 90$ deg. The geometry for typical distant sources is schematically illustrated in Fig. 3. For the (extreme) range of geometry illustrated in Fig. 3, the expected approximate contribution (Δ) to the total power law radial dependence would be:

$$\Delta \approx \frac{\ell n\left(\frac{\beta_1}{\beta_2}\right)}{\ell n\left(\frac{a_1}{a_2}\right)} = \frac{\ell n\left(\frac{90}{153}\right)}{\ell n\left(\frac{215}{96}\right)} = -0.7$$

so that one would expect the data to display a total radial dependence of $\approx a^{-2.0}$, under the assumption of a signal path integration of a $Kr^{-2.3}$ source function. Possible interplanetary scintillation examples of this expected exaggerated steepening of the total radial dependence as β approaches 90° are the 81.5 MHz data of Fig. 3 in Rickett (Ref. 13), and the 73.8 MHz data of Fig. 1 in Coles, et al., (Ref. 14). The 81.5 MHz data from Rickett extend over the region 117 $r_o < a < 215$ r_o and do in fact display a total radial dependence of $\approx a^{-2.0}$, according to the published fit line in Ref. 13.

For natural sources (interplanetary scintillation) only the "near-Earth" limit is a geometrical consideration, whereas in the case of man-made (spacecraft) sources, the geometry will be a combination of the "near-Earth" and "near-source" effects.

IV. Application of the Total Radial Dependence Concept

To further explore the concept of "total" radial dependence, one can utilize the Doppler phase fluctuation (Doppler scintillation) data in Woo (Ref. 1). These data are for all intents and purposes the same as data published earlier in Berman, et al. (Ref. 4). Since Berman found these data compatible with the signal path integration of a $Kr^{-2.3}$ source, one would expect Ref. 1 to find a total radial dependence of approximately $a^{-1.5}$. In Fig. 11 of Ref. 1 (reproduced here as Fig. 2), the data are shown with a fit line of $a^{-1.45}$, in reasonable accordance with expectations; however, the line is mislabeled as $a^{-1.3}$. Subsequently, Woo has republished (Ref. 15) these data with a new, correct $a^{-1.3}$ fit line (also reproduced here in Fig. 2). Visual inspection of the two fits seen in Fig. 2 clearly favors the original (mislabelled) $a^{-1.45}$ fit.

V. Discussion and Summary

Solar wind columnar turbulence results from the signal path integration of an appropriate solar wind parameter, and hence two independent geometrical parameters are required to provide a complete and accurate functional description. The two most appropriate geometrical parameters are the Sun-Earth-probe angle and Earth-Sun-probe angle. Attempts to model experimental measurements of solar wind columnar turbulence as a function of only a single geometrical parameter (e.g., Sun-Earth-probe angle, the dominant parameter) are inherently less accurate than using a complete geometrical description, and serve to mask the proper experimental relationship between columnar turbulence and the signal path integration of an appropriate source function.

Because of the preponderance of evidence linking columnar turbulence with the signal path integration of a power-law electron density model, this article has undertaken to quantify the distortion resulting from reliance on a single geometrical parameter, and to establish an approximate relationship between "total" radial dependence and the signal path integration of a power law source function. The net effect of reliance on a single geometric parameter is to (very approximately) translate the correct two parameter formulation:

$$\phi(a,\beta) \cong K \beta a^{-1.3} F(a,\beta)$$

into a considerably less accurate expression of the form:

$$\phi(a) \approx K a^{-1.5}$$

For future experimental measurement and modelling of solar wind columnar turbulence, usage of a two geometrical parameter model based on the signal path integration of a power law source function is clearly indicated.

References

1. Woo, R., "Radial Dependence of Solar Wind Properties Deduced from Helios 1/2 and Pioneer 10/11 Radio Scattering Observations," in *The Astrophysical Journal 219,* January 15, 1978.

2. Callahan, P. S., "An Analysis of Viking S-X Doppler Measurements of Solar Wind Columnar Content Measurements," in *The Deep Space Network Progress Report 42-44,* Jet Propulsion Laboratory, Pasadena, California, 15 April 1978.

3. Berman, A. L., Wackley, J. A., and Hietzke, W. H., "The First Direct Comparison of Doppler Phase Fluctuation to Integrated Electron Density Over an Extensive Span of Signal Closest Approach Distance – A Brief Report," IOM ALB-78-35, March 10, 1978 (a JPL internal document).

4. Berman, A. L., and Wackley, J. A., "Doppler Noise Considered as a Function of the Signal Path Integration of Electron Density," in *The Deep Space Network Progress Report 42-33,* Jet Propulsion Laboratory, Pasadena, California, 15 June 1976.

5. Erskine, F. T., Cronyn, W. M., Shawhan, S. D., Roelof, E. C., and Gotwols, B. L., "Interplanetary Scintillation at Large Elongation Angles: Reponse to Solar Wind Density Structure," in *The Journal of Geophysical Research,* Volume 83, Number A9, September 1, 1978.

6. Chang, H., *Analysis of Dual-Frequency Observations of Interplanetary Scintillations Taken by the Pioneer 9 Spacecraft,* Doctoral Dissertation, Department of Electrical Engineering, Stanford University, May 1976.

7. Houminer, Z., and Hewish. A., "Correlation of Interplanetary Scintillation and Spacecraft Plasma Density Measurements," in *Planetary and Space Science,* Volume 22, Number 6, June 1974.

8. Berman, A. L., "Electron Density in the Extended Corona: Two Views," in *The Deep Space Network Progress Report 42-41,* Jet Propulsion Laboratory, Pasadena, California, 15 October 1977.

9. Berman, A. L., "Electron Density and Doppler RMS Phase Fluctuation in the Inner Corona," in *The Deep Space Network Progress Report 42-44,* Jet Propulsion Laboratory, Pasadena, California, 15 April 1978.

10. Berman, A. L., "Solar Wind Turbulence Models Evaluated via Observations of Doppler RMS Phase Fluctuation and Spectral Broadening in the Inner Corona," in *The Deep Space Network Progress Report 42-44,* Jet Propulsion Laboratory, Pasadena, California, 15 April 1978.

11. Rockwell, S. T., "An Empirical Spectral Bandwidth Model for Superior Conjunction," in *The Deep Space Network Progress Report 42-43,* Jet Propulsion Laboratory, Pasadena, California, 15 February 1978.

12. Berman, A. L., Wackley, J. A., Rockwell, S. T., and Kwan, M., "Viking Doppler Noise Used to Determine the Radial Dependence of Electron Density in the Extended Corona," in *The Deep Space Network Progress Report 42-38,* Jet Propulsion Laboratory, Pasadena, California, 15 April 1977.

13. Rickett, B. J., "Power Spectrum of Density Irregularities in the Solar Wind Plasma," in *The Journal of Geophysical Research,* Volume 78, Number 10, April 1, 1973.

14. Coles, W. A., Rickett, B. J., and Rumsey, V. H., "Interplanetary Scintillations," in *Solar Wind Three,* edited by Russell, C. T., published by the Institute of Geophysics and Planetary Physics, University of California, Los Angeles, California, July 1974.

15. Woo, R. "Errata," in *The Astrophysical Journal* 223, July 15, 1978.

Table 1. Relationship of signal path integrated density model of radial (power law) index $-(2 + \xi)$ to total (power law) radial dependence

Spacecraft	Year	Data span of (a/r_o)	Data span of β, deg	ξ	$\frac{\ln(\beta_1/\beta_2)}{\ln(a_1/a_2)}$	"Total" radial dependence
Pioneer 10	1975	17–170	174.8–121.4	0.3	−0.16	-1.46
Pioneer 11	1975	17–170	174.5–116.6	0.3	−0.18	-1.48
Helios 1	1975	12–60	171.5–102.7	0.3	−0.32	-1.62
Viking	1976	17–170	172.5–98.9	0.3	−0.24	-1.54
Average					−0.22	-1.52

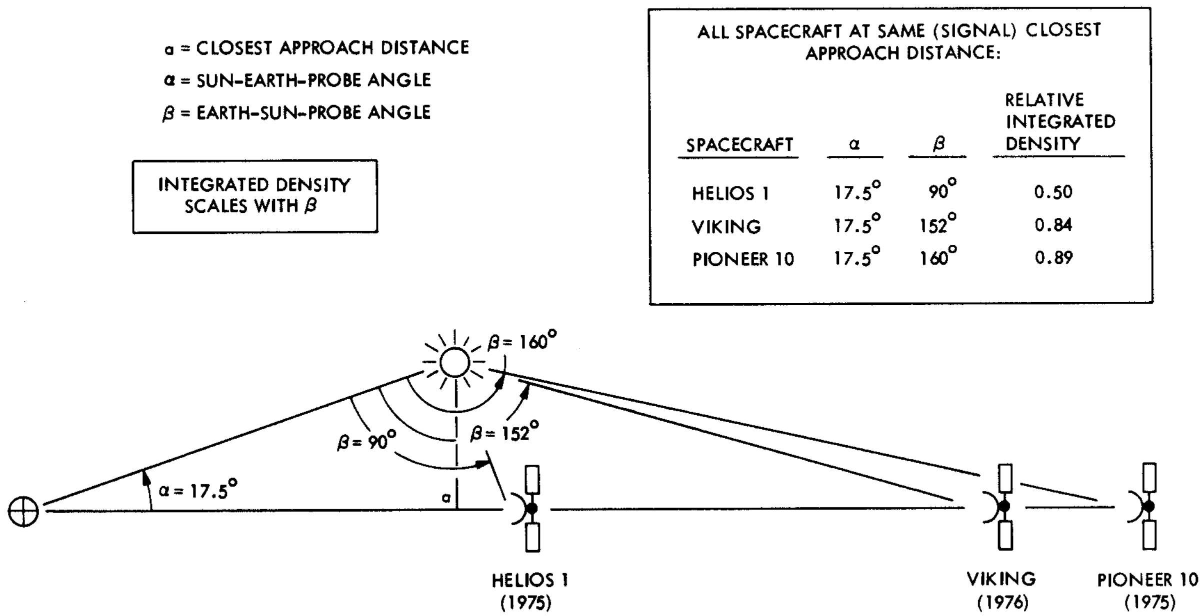

SPACECRAFT	α	β	RELATIVE INTEGRATED DENSITY
HELIOS 1	17.5°	90°	0.50
VIKING	17.5°	152°	0.84
PIONEER 10	17.5°	160°	0.89

Fig. 1. Integrated density reduction for spacecraft due to "near-source" limit

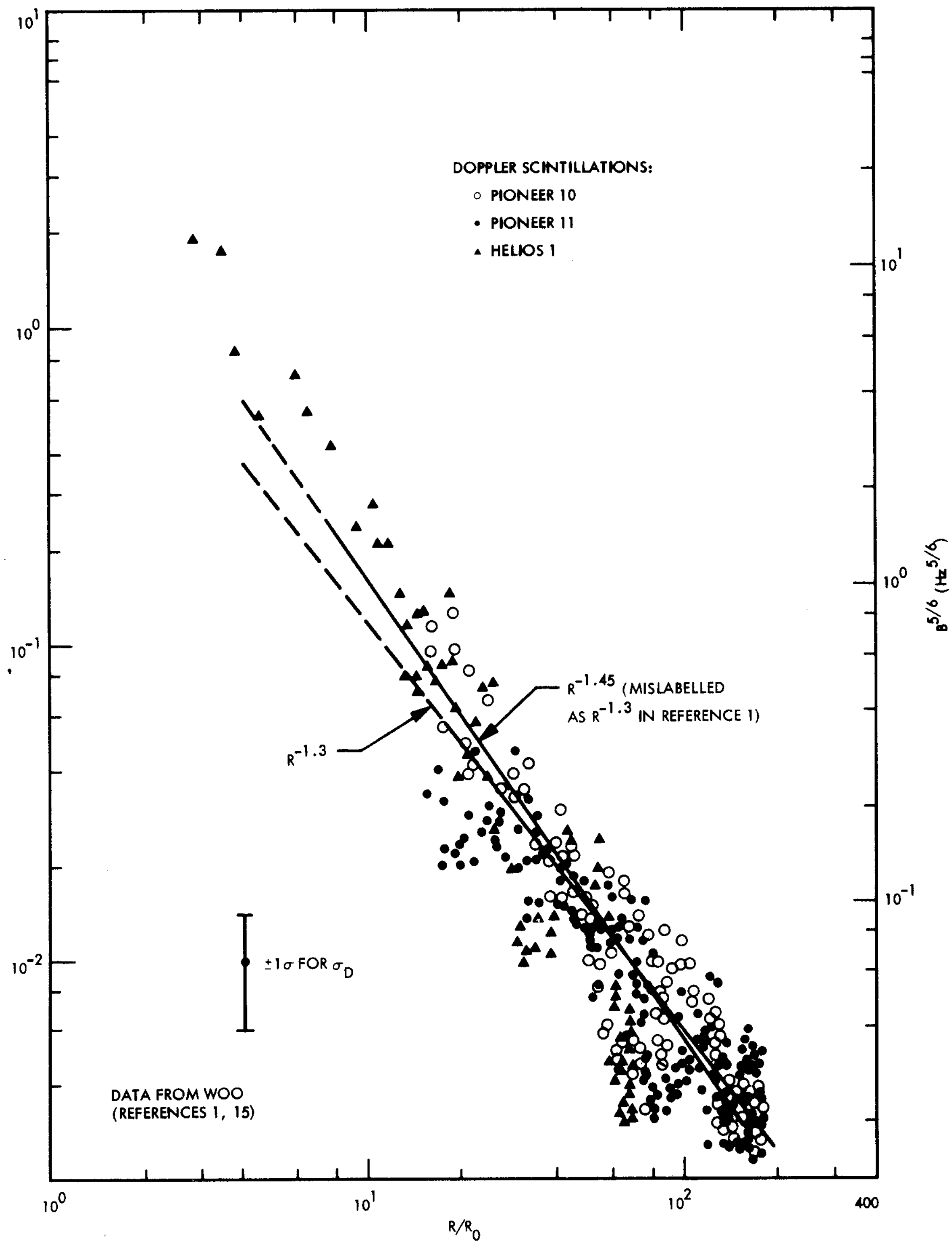

Fig. 2. Doppler phase fluctuation versus radial distance

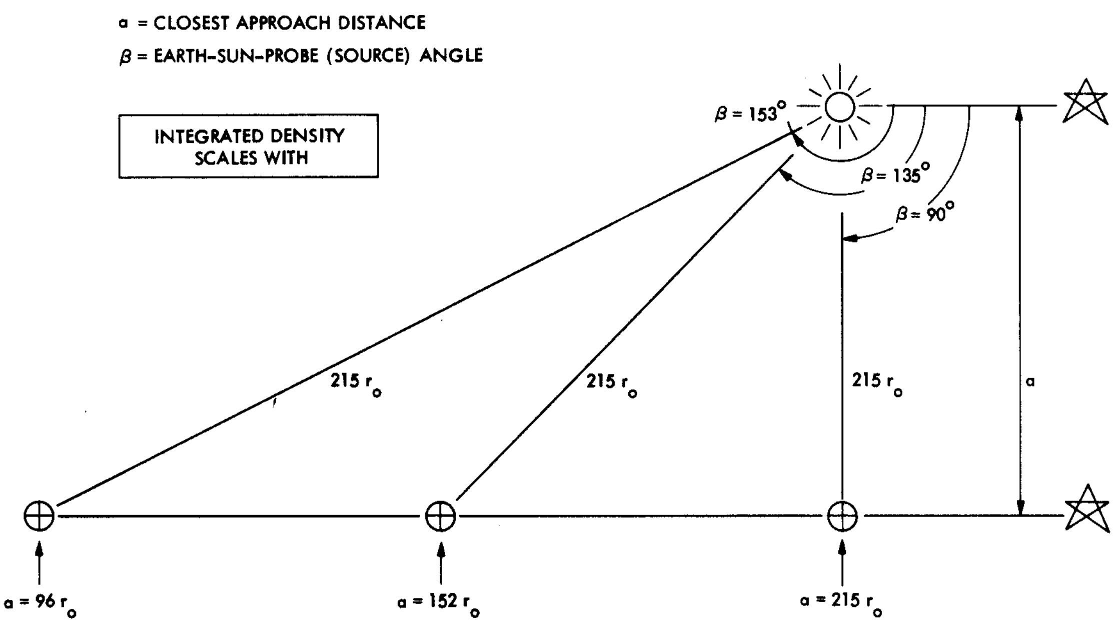

Fig. 3. Integrated density reduction for distant spacecraft and natural sources due to "near Earth" limit